Subscriber access provided by ISTANBUL TEKNIK UNIV

JACS
JOURNAL OF THE AMERICAN CHEMICAL SOCIETY

Communication

Battery-Inspired, Nonvolatile, and Rewritable Memory Architecture: a Radical Polymer-Based Organic Device

Yasunori Yonekuta, Kentaro Susuki, Kenichi Oyaizu, Kenji Honda, and

J. Am. Chem. Soc., **2007**, 129 (46), 14128-14129• DOI: 10.1021/ja075553p • Publication Date (Web): 27 October 2007

Downloaded from http://pubs.acs.org on February 13, 2009

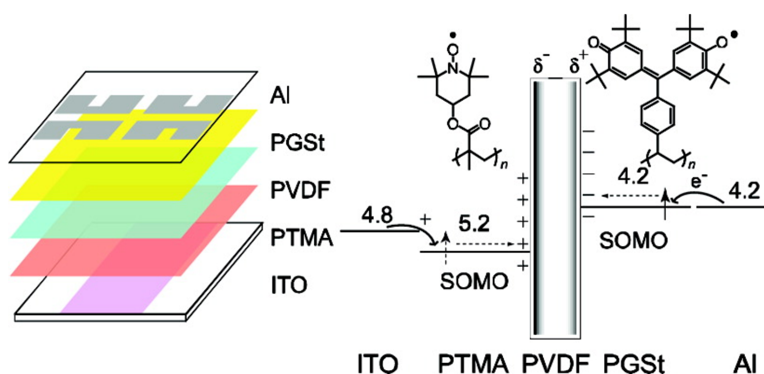

More About This Article

Additional resources and features associated with this article are available within the HTML version:

- Supporting Information
- Links to the 4 articles that cite this article, as of the time of this article download
- Access to high resolution figures
- Links to articles and content related to this article
- Copyright permission to reproduce figures and/or text from this article

View the Full Text HTML

ACS Publications
High quality. High impact.

Journal of the American Chemical Society is published by the American Chemical Society. 1155 Sixteenth Street N.W., Washington, DC 20036

J|A|C|S
COMMUNICATIONS

Published on Web 10/27/2007

Battery-Inspired, Nonvolatile, and Rewritable Memory Architecture: a Radical Polymer-Based Organic Device

Yasunori Yonekuta, Kentaro Susuki, Kenichi Oyaizu, Kenji Honda, and Hiroyuki Nishide*

Department of Applied Chemistry, Waseda University, Tokyo 169-8555, Japan

Received July 25, 2007; E-mail: nishide@waseda.jp

Organic robust polyradicals are establishing their position as a new class of functional polymers, such as ferromagnetic materials, based on the spin alignment of unpaired electrons through conjugated backbones.[1] An intriguing aspect of the current research is the application of radical polymers, i.e., aliphatic polymers bearing redox-active radical pendant groups, to high capacity charge-storage materials for secondary batteries.[2] The high power characteristics of the so-called "radical battery" originate from the large heterogeneous electron-transfer rate of the redox centers and the efficient mass-transfer process within the polymer layers, allowing facile accommodation of electrolyte ions to compensate charges generated from the neutral radicals. Nernstian electrochemical behaviors have been found for a number of robust radicals, such as the 1e− oxidation of 2,2,6,6-tetramethylpiperidine-1-oxyl (TEMPO) to the oxoammonium cation and the 1e− reduction of galvinoxyl radicals to the galvinolate anion.[3] Radical polymers bearing pendant TEMPO and galvinoxyl groups undergo heavy p- and n-doping and are used as cathode- and anode-active materials in the radical battery, respectively, by sandwiching an electrolyte layer. We anticipated that a similar charge-storage configuration should develop for a dry system in the absence of the electrolyte layer, by sandwiching a dielectric material with the radical polymers. The expected result is an electroconductive bistability, rather than the power storage. Here we report the excellent properties of an organic "radical memory", which provided insight into the mechanism of charge storage at an electrode interface under dry conditions.

The organic-based memory was first introduced for FeRAM-type devices, wherein fluorine-containing polymers were used as the dielectric material to replace silicon dioxide in combination with inorganic semiconductor-based transistors.[4] All plastic-type memory systems have attracted recent attention as a new type of low voltage-driven memory between conventional DRAM/SRAM devices and magnetic hard discs, in addition to the inherent advantages allowing for a facile wet-process fabrication. Several types of organic materials have been examined for this purpose, such as organic semiconductors,[5−7] charge-transfer complexes,[8,9] redox-active compounds, and metal nanoparticle-dispersed thin films.[10,11] However, the organic-based devices often fell into write-once-read-many type memory characteristics and suffered from a low ON−OFF ratio remaining at less than 2 orders of magnitude. We selected structure-defined radical polymers which yielded contamination-free, homogeneous, and tough organic layers for improvement of the device behaviors.

The metal−insulator−metal diode-type structure of the fabricated radical memory is shown in Figure 1. The device was composed of the thin layers of poly(2,2,6,6-tetramethylpiperidine-1-oxyl methacrylate) (PTMA) as the p-type redox active material, polyvinylidene difluoride (PVDF) as the dielectric material, and poly(4-(2,6-di-*tert*-butyl-α-(3,5-di-*tert*-butyl-4-oxo-2,5-cyclohexadien-1-ylidene)-*p*-tolyloxy)styrene) (PGSt) as the n-type redox activate

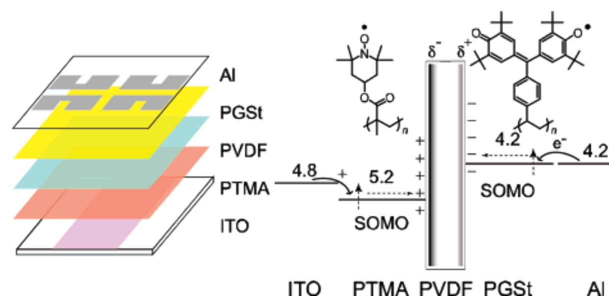

Figure 1. Radical polymer-based memory architecture and charge injection, transporting, and trapping mechanism at the PVDF interfaces, and energy level diagram for the ITO, PTMA, PGSt, and Al.

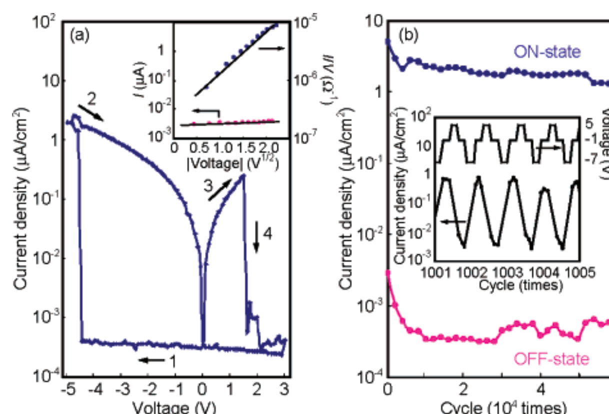

Figure 2. (a) $I-V$ characteristics of the device with an ITO/PTMA/PVDF/PGSt/Al configuration. Inset: Analysis of $I-V$ characteristics for the device in the ON (●) and OFF (○) states. The ON- and OFF-state responses were fitted for the Poole−Frenkel emission and Schottky effects, respectively. (b) Retention cycle tests for current density at −1 V after pulse applications at the write voltage of −7 V (blue circles) and the erase voltage of 5 V (red circles). Inset: Endurance test results during the application of write-, read-, and erase-voltage cycles.

material. These layers were conveniently spin-coated onto an ITO/glass electrode from solutions of PTMA in ethyl lactate, PVDF in hexamethylphosphoramide, and PGSt in toluene. The polymer multilayer was successfully formed without substantial intermixing, by virtue of the significant difference in solubility. An AFM image of the PTMA layer on the ITO substrate (Figure S1) revealed a highly smooth and homogeneous surface with a mean roughness of 1 nm, although the ITO surface had a larger roughness of ca. 10 nm. The effects of the depletion defects and pinholes are thus likely to be excluded for the polymer-based devices. The top Al electrode had a width of 5 mm, so that the device had a measured area of 25 mm^2.

The typical $I-V$ characteristics of the device are shown in Figure 2a. When an increasing voltage of 0 to −5 V was applied to the Al electrode versus the ITO electrode (sweep 1), the state of the device was precipitously switched to low resistance near −4.5 V

10.1021/ja075553p CCC: $37.00 © 2007 American Chemical Society

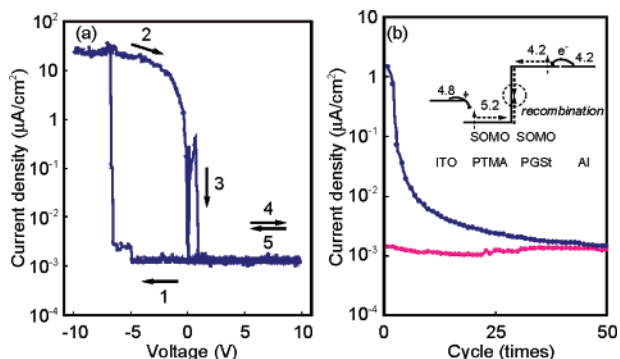

Figure 3. (a) $I-V$ characteristics of the rectifying device with a configuration of ITO/PTMA/PGSt/Al (see Figure S3). (b) Retention cycle tests by applying the pulses in the order of V_W and V_R (ON state, ●), or V_E and V_R (OFF state, ○), consecutively. Inset: Energy level diagram for the rectifying device.

as the threshold voltage. The low-resistance state was maintained during the reverse sweep of the voltage from −5 to 1.4 V (sweeps 2 and 3 in Figure 2a). The low-resistance or ON state was observed for repeated sweeps, regardless of the sweep direction (Figure S2a). When a bias of ca. 1.5 V was applied, the device sharply switched to the high-resistance or OFF state again (sweep 4). In the hysteretic curve, the ON−OFF ratio amounted to 4 orders of magnitude. The optimum write (V_W), erase (V_E), and read voltages (V_R) were determined to be −7, 5, and −1 V, respectively. The results of the retention and endurance cycle tests for switching between the ON and OFF states are shown in Figure 2b. The current for the OFF state after the V_E pulse for 0.1 s, detected by the V_R pulse with a current of 10^{-3} μA, was significantly smaller than that for the ON state after the V_W pulse for 0.1 s (100 μA). The retention cycles of the ON and OFF states under open-circuit conditions persisted for more than 10^4 times. Furthermore, each state survived for a month after the corresponding once-time-only pulse as well as consecutive pulses. Endurance tests were similarly performed by consecutively applying the pulses in the order of V_W, V_R, V_E, and V_R. The slight decay of the ON−OFF ratio might be caused by slow degradation of the device. However, the repeatable performance was confirmed for more than 10^3 cycles.

Control experiments using a PVDF-free device with a configuration of ITO/PTMA/PGSt/Al (Figure 3a) revealed the origin of the ON-state stability. The negative bias applied to the pristine highly resistant device induced a similar transition to the low-resistant state (sweeps 1 and 2). However, the resulting ON state was quenched by applying any positive bias (sweep 3). The ON-state current gradually decreased and converged to that of the OFF state after 50 sweeps (Figure 3b). A plausible mechanism based on these result is a rectification effect of the p−n junction where charge consumption by recombination prevails at the PTMA/PGSt interface (Figure 3b, inset). The lack of any current from the positively biased device (sweeps 4 and 5) suggests the absence of the trapped charges in the polymer layers.

The Schottky effect and the Poole−Frenkel (PF) emission are anticipated for the charge injection at the radical polymer/electrode interface and the charge transfer within the radical polymer layer, respectively.[12−14] As shown in Figure 2a, the plots of log(I) versus $V^{1/2}$ were linear in the high-resistance range of 0 to −4.5 V before the electrical transition, which indicated that the OFF state was dominated by the Schottky barrier or the charge-injection process. On the other hand, the $I-V$ plots for the ON state obeyed a linear log(I/V) versus $V^{1/2}$ relationship, suggesting that the PF emission was responsible for the charge transfer (see Figure 2a). In the ON state, charges were trapped at the radical polymer/PVDF interfaces, which induced accumulation of the opposite charges at the radical polymer/electrode interfaces and reduced the Schottky barriers, allowing charges to transfer across the radical polymer/electrode interfaces even at low voltages.

The SOMO levels of PTMA and PGSt were 5.2 and 4.2 eV, respectively. The PTMA layer accepts holes from the ITO, and electrons are injected into the PGSt layer from Al. The injected holes and electrons are transported by the hopping mechanism and are stored at the radical polymer/PVDF interfaces. Under open circuit conditions, the trapped holes and electrons were nonvolatile due to not only the charge trapping at the radical polymer/PVDF interfaces but also the blocking of the charge transfer in the PTMA and PGSt layers having sufficient resistances. The asymmetric configuration of the electrodes with the different work functions allows initialization of the device by applying an inverse voltage.

In conclusion, the battery-inspired PTMA/PVDF/PGSt configuration led to the unique electroconductive bistability that functions as the memory device. Our preliminary impedance experiments have suggested that the device operates at a frequency of up to 10^5 Hz indicating a high rate of switching for the ON−OFF transition, which are the topics of our continuous research.

Acknowledgment. This work was partially supported by Grants-in-Aid for Scientific Research (Nos. 19105003, 17067017) and the Global COE Program from MEXT, Japan.

Supporting Information Available: Materials, measurements, synthesis, and additional experiments. This material is available free of charge via the Internet at http://pubs.acs.org.

References

(1) (a) *Magnetic Properties of Organic Materials*; Lahti, P. M., Ed.; Marcel Decker: New York, 1999. (b) Rajca, A.; Wongsriratanakul, J.; Rajca, S. *Science* **2001**, *294*, 1503. (c) *Carbon-Based Magnetism*; Makaroba, T., Palacio, F., Ed.; Elsevier: Amsterdam, 2006. (d) Kaneko, T.; Makino, T.; Miyaji, H.; Teraguchi, M.; Aoki, T.; Miyasaka, M.; Nishide, H. *J. Am. Chem. Soc.* **2003**, *125*, 3554. (e) Fukuzaki, E.; Nishide, H. *J. Am. Chem. Soc.* **2006**, *128*, 996.

(2) (a) Nishide, H.; Suga, T. *Electrochem. Soc. Interface* **2005**, *14*, 32. (b) Suga, T.; Konishi, H.; Nishide, H. *Chem. Commun.* **2007**, *17*, 1730. (c) Suga, T.; Pu, Y.-J.; Kasatori, S.; Nishide, H. *Macromolecules* **2007**, *40*, 3167.

(3) Yonekuta, Y.; Oyaizu, K.; Nishide, H. *Chem. Lett.* **2007**, *36*, 866.

(4) Stikeman, A. *Tech. Rev.* **2002**, *105*, 31.

(5) Möller, S.; Perlov, C.; Jackson, W.; Taussig, C.; Forrest, S. R. *Nature* **2003**, *426*, 166.

(6) Tondelier, D.; Lmimouni, K.; Vuilaume, D. *Appl. Phys. Lett.* **2004**, *85*, 5763.

(7) Bozano, L. D.; Kean, B. W.; Deline, V. R.; Salem, J. R.; Scott, J. C. *Appl. Phys. Lett.* **2004**, *84*, 607.

(8) (a) Potember, R. S.; Poehler, T. O.; Cowan, D. O. *Appl. Phys. Lett.* **1979**, *34*, 405. (b) Oyamada, T.; Tanaka, H.; Matsushige, K.; Sasabe, H.; Adachi, C. *Appl. Phys. Lett.* **2003**, *83*, 1252.

(9) (a) Ling, Q. D.; Song, Y.; Ding, S. J.; Zhu, C. X.; Chan, D. S. H.; Kwong, D. L.; Kang, E. T.; Neoh, K. G. *Adv. Mater.* **2005**, *17*, 455. (b) Song, Y.; Ling, Q. D.; Zhu, C. X.; Kang, E. T.; Chan, D. S. H.; Wang, Y. H.; Kwong, D. L. *IEEE Electron. Device Lett.* **2006**, *27*, 154. (c) Ling, Q. D.; Song, Y.; Lim, S. L.; Teo, E. Y. H.; Tan, Y. P.; Zhu, C. X.; Chan, D. S. H.; Kwong, D. L.; Kang, E. T.; Neoh, K. G. *Angew. Chem., Int. Ed.* **2006**, *45*, 2947.

(10) Gofer, Y.; Sarker, H.; Killian, J. G.; Poehler, T. O.; Searson, P. C. *Appl. Phys. Lett.* **1997**, *71*, 1582.

(11) Tseng, R. J.; Huang, J.; Ouyang, J.; Kaner, R. B.; Yang, Y. *Nano Lett.* **2005**, *5*, 1077.

(12) Laurent, C.; Kay, E.; Souag, N. *J. Appl. Phys.* **1988**, *64*, 336.

(13) Vollmann, W.; Poll, H.-U. *Thin Solid Films* **1975**, *26*, 201.

(14) Chu, C. W.; Ouyang, J.; Tseng, J.-H.; Yang, Y. *Adv. Mater.* **2005**, *17*, 1440.

JA075553P